

## Are long gamma-ray bursts progenitors to merging binary black holes?

TOM Y. WU<sup>1</sup> AND MAYA FISHBACH<sup>2,1,3</sup>

<sup>1</sup>*David A. Dunlap Department of Astronomy and Astrophysics, University of Toronto, 50 St George St, Toronto ON M5S 3H4, Canada*

<sup>2</sup>*Canadian Institute for Theoretical Astrophysics, 60 St George St, University of Toronto, Toronto, ON M5S 3H8, Canada*

<sup>3</sup>*Department of Physics, 60 St George St, University of Toronto, Toronto, ON M5S 3H8, Canada*

### ABSTRACT

The distribution of delay times between the formation of binary black hole (BBH) progenitors and their gravitational-wave (GW) merger provides important clues about their unknown formation histories. When inferring the delay time distribution, it is typically assumed that BBH progenitor formation traces the star formation rate (SFR). In this work, we consider the rate of long gamma-ray bursts (LGRBs) instead of the SFR. LGRBs are thought to correspond to the formation of (possibly spinning) black holes, and may therefore be related to the population of BBH progenitors. By comparing the redshift evolution of the LGRB rate as inferred by Ghirlanda & Salvaterra (2022) and the BBH merger rate inferred by LIGO-Virgo-KAGRA (LVK) observations, we find that the delay time distribution between LGRBs and BBH mergers is well-described by a power law with minimum delay time 10 Myr and slope  $\alpha = -0.96_{-0.85}^{+0.64}$  (90% credibility). This matches theoretical predictions for the BBH delay time distribution, which in turns lends support to the hypothesis that LGRBs trace BBH progenitor formation. However, comparing the absolute rates of these two populations, we find that at most  $f = 0.04_{-0.03}^{+0.18}$  of LGRBs may evolve into merging BBH. We also consider the possibility that LGRBs only produce BBH systems with large aligned spins (with effective inspiral spin  $\chi_{\text{eff}} > 0.2$ ). In this case, we find  $f = 0.003_{-0.002}^{+0.011}$  and the delay time distribution favors the steepest power law slopes we consider ( $\alpha = -2$ ).

### 1. INTRODUCTION

There are many proposed evolutionary channels for making merging binary black hole (BBH) systems (see, e.g., Mapelli 2020; Mandel & Farmer 2022, for reviews). Merging BBH systems likely evolve from massive stars that collapse into black holes (BHs) at the end of their lives. Under rare conditions, binary star evolution and/or stellar dynamics causes a BH stellar remnant to end up in a tight binary with another BH. If the binary is sufficiently tight, its orbit decays due to gravitational-wave (GW) radiation and the two BHs inspiral towards each other and finally merge into one. It often takes billions of years for two BHs to merge due to GW radiation, because the inspiral time  $\tau_{\text{insp}}$  strongly depends on the initial orbital separation  $a$ ; for circular binaries,  $\tau_{\text{insp}} \propto a^4$  (Peters 1964). Because massive stars die so quickly ( $\lesssim 10$  Myr), the delay time  $\tau$  between the formation of the progenitor stars and the merger of the BBH system is almost entirely dominated by the GW inspiral phase,  $\tau \approx \tau_{\text{insp}}$ . This delay time depends on the initial binary orbit, and thus on the astrophysical processes responsible for creating the BBH system. By measuring the delay time distribution for the BBH population, we

gain insight into the formation of merging BBHs. Many formation channels predict delay time distributions that are well-described as a power law  $p(\tau) \propto \tau^\alpha$  with slopes  $-1.5 \lesssim \alpha \lesssim -0.3$  (e.g. O’Shaughnessy et al. 2010; Dominik et al. 2012; Rodriguez & Loeb 2018; Mapelli et al. 2019; Di Carlo et al. 2020; Fishbach & van Son 2023; Ye & Fishbach 2024; Boesky et al. 2024).

In the past decade, the GW detector network consisting of LIGO, Virgo and KAGRA (LIGO Scientific Collaboration et al. 2015; Acernese et al. 2015; Akutsu et al. 2021) has observed the GW radiation from  $\mathcal{O}(100)$  BBH mergers. The third Gravitational-Wave Transient Catalog GWTC-3 (Abbott et al. 2023) includes  $\approx 70$  confident BBHs (with false-alarm rate FAR  $< 1$  per year). Previous studies (Fishbach & Kalogera 2021; Vijaykumar et al. 2023; Turbang et al. 2024; Schiebelbein-Zwack & Fishbach 2024) used these events to infer the BBH delay time distribution by comparing the redshift evolution of the BBH merger rate to the star formation rate (SFR). This assumes that the progenitors of BBH mergers trace the SFR. However, BBH progenitors are likely biased tracers of star formation because the fraction of stars that produce merging BBH systems depends on conditions that vary over cosmic time,

like the metallicity, the stellar initial mass function, and the binary fraction (e.g. [Belczynski et al. 2010](#); [Klencki et al. 2018](#); [Santoliquido et al. 2021](#); [Chruślińska 2024](#); [Boesky et al. 2024](#)). Earlier studies that measured the BBH delay time distribution therefore included a metallicity-dependent formation efficiency, effectively assuming that BBH progenitors trace the low-metallicity SFR. This introduces additional uncertainty because the low-metallicity SFR is not well known (see, e.g. [Chruślińska 2024](#), for a review of the effect on GW populations). Nevertheless, assuming reasonable values of the metallicity-specific SFR from observations (e.g. [Madau & Fragos 2017](#)) and the metallicity-dependent BBH formation efficiency from theoretical models (e.g. [Dominik et al. 2013](#)), the BBH delay time distribution was inferred to strongly favor short delay times (power law slopes  $\alpha < -1$ ; [Turbang et al. 2024](#); [Schiebelbein-Zwack & Fishbach 2024](#)), in tension with some theoretical predictions ([Fishbach & van Son 2023](#)).

As an alternative to the (low-metallicity) SFR, long gamma-ray bursts (LGRBs), which are commonly associated with the collapse of massive stars into black holes, may better trace BBH progenitors. Observationally, LGRBs are associated with sub-solar metallicity environments ([Vergani et al. 2015](#); [Perley et al. 2016a](#); [Palmerio et al. 2019](#)). LGRB jets are thought to be powered by the rotation of the collapsing stellar core (“collapsar;” [Woosley 1993](#); [MacFadyen & Woosley 1999](#)). The mechanism by which massive stars maintain significant core rotation may be related to BBH evolutionary pathways.

Indeed, [Bavera et al. \(2022b\)](#) recently proposed that the origin of (some) LGRBs is linked to the formation of BBH mergers with spinning component BHs. They postulate that sufficiently rotating stellar cores are created from tight binaries (e.g. tidal spin-up in post common envelope systems or chemically homogeneous binary star evolution) that are also oftentimes the progenitors of BBH mergers. Unless launching the LGRB spins down the BH ([Jacquemin-Ide et al. 2024](#)), the BBH system would also contain one (in the tidal spinup case) or two (in the chemically homogeneous evolution case) spinning component BH in this scenario. [Bavera et al. \(2022b\)](#) combine their population synthesis models with GW observations from GWTC-2 and LGRB observations from the SHOALS survey ([Perley et al. 2016b](#)), inferring that  $\sim 10\%$  of observed BBH mergers had an associated LGRB earlier in their evolution, and 20–85% of LGRBs may have an associated BBH merger later in their evolution. On the other hand, [Arcier & Atteia \(2022\)](#) analyzed GW and LGRB observations and concluded that BBH mergers cannot come from LGRB

progenitors unless they experience long delay times of several Gyrs.

In this work, we revisit the [Arcier & Atteia \(2022\)](#) analysis and compare the populations of LGRBs and BBH mergers. Using the GWTC-3 observations, we infer the BBH delay time distribution assuming that their progenitors follow the LGRB rate as measured by [Ghirlanda & Salvaterra \(2022\)](#), scaled by some factor. Over the currently observable range of BBH merger redshifts  $0 < z < 1$ , the BBH merger rate evolves slightly less steeply than the LGRB rate. Therefore, contrary to [Arcier & Atteia \(2022\)](#), we find that the BBH merger rate is consistent with tracing the LGRB rate with relatively short delay times, consistent with population synthesis predictions. Our findings therefore support LGRBs as tracers of the BBH progenitor formation rate based on the shape of their redshift evolution. However, BBH progenitors can make up only a small fraction of the LGRB rate, which is  $\mathcal{O}(10)$  times higher than the BBH progenitor rate. We also repeat our analysis under the assumption that only BBH mergers with significant aligned spins originate from LGRBs, in which case the delay time distribution may be steeper (favoring shorter delays).

## 2. METHODS

### 2.1. Applying delay time distributions to the LGRB rate

For a given formation rate  $\mathcal{R}_f$  and delay time distribution  $p(\tau)$ , the merger rate at a lookback time  $t_L$  is given by:

$$\mathcal{R}_m(t_L) = \int_{\tau_{\min}}^{\tau_{\max}} \mathcal{R}_f(t_L + \tau)p(\tau)d\tau, \quad (1)$$

where  $\tau_{\min}$  and  $\tau_{\max}$  are the minimum and maximum delay times, respectively. We assume that the maximum redshift of progenitor formation is  $z = 15$ , corresponding to a lookback time of 13.519 Gyr, which we also fix as the maximum delay time,  $\tau_{\max} = 13.519$  Gyr. (We use the best fit cosmological parameters from [Planck Collaboration et al. 2020](#) throughout, as implemented by [ASTROPY \(Astropy Collaboration et al. 2013, 2022\)](#)). The BBH delay time distribution is often modeled as a power law with power-law slope  $\alpha$ :

$$p(\tau|\alpha) = \tau^\alpha \cdot \frac{\alpha + 1}{\tau_{\max}^{\alpha+1} - \tau_{\min}^{\alpha+1}} \quad (2)$$

In [Fig. 1](#), we show some examples of the merger rate corresponding to a progenitor formation rate given by the best-fitting LGRB rate  $\mathcal{R}_f \equiv \mathcal{R}_{\text{LGRB}}$  from [Ghirlanda & Salvaterra \(2022\)](#) convolved with a few different power-law delay time distributions varying  $\alpha$

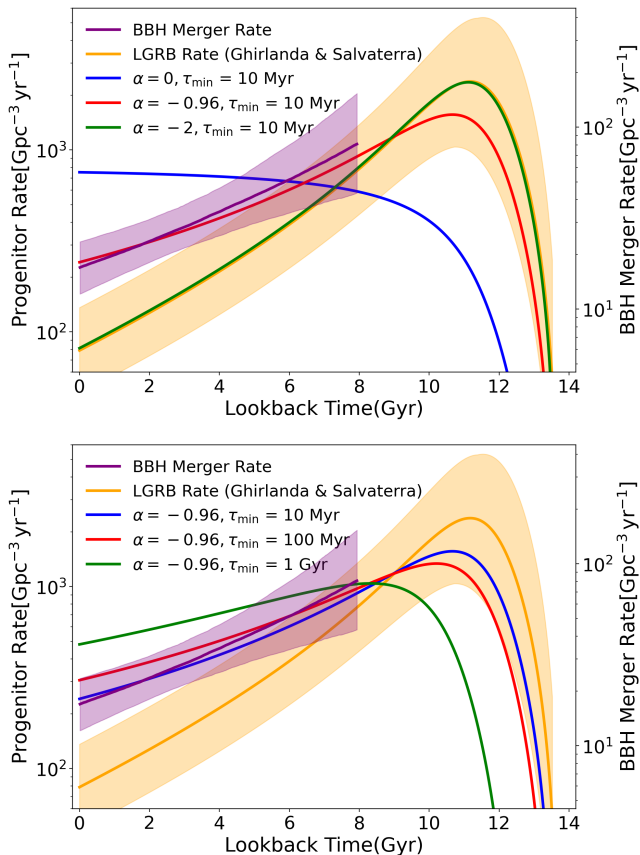


**Figure 1.** Upper panel: In orange (left axis), the maximum likelihood LGRB rate and its uncertainty from Ghirlanda & Salvaterra (2022). The LGRB rate peaks at redshift  $z = 2.6$ , which corresponds to a lookback time  $t_L = 11.2$  Gyr. Blue, red and green curves show the predicted BBH merger rates assuming the maximum likelihood value of  $\mathcal{R}_{\text{LGRB}}$  for the formation rate and power-law delay time distributions with  $\alpha = 0, -0.96, -2$ , respectively (at  $\tau_{\min} = 10$  Myr,  $-0.96$  is our best prediction for  $\alpha$ , as we will derive in later sections). In purple (right axis) is the BBH merger rate inferred by Bavera et al. (2022a). Lower panel: Same as above, fixing  $\alpha = -0.96$  and taking different values of  $\tau_{\min}$  from 10 Myr (blue), 100 Myr (red) and 1 Gyr (green).

(top panel) and  $\tau_{\min}$  (bottom panel). The LGRB rate is shown in orange, with shaded bands denoting 68% uncertainty. For the uncertainty on  $\mathcal{R}_{\text{LGRB}}$ , we use the reported one-dimensional (marginal) uncertainties on the inferred LGRB rate parameters from Ghirlanda & Salvaterra (2022), but we neglect correlations between the parameters, so our uncertainty bands are more conservative than the results of Ghirlanda & Salvaterra (2022). Delay time distributions with more negative  $\alpha$  or smaller  $\tau_{\min}$  favor shorter delay times, yielding predicted merger rates that are closer to the LGRB rate. In fact, a delay time distribution with  $\alpha = -2$  and  $\tau_{\min} = 10$  Myr (green line in the top panel of Fig. 1) is nearly indistinguishable

from the LGRB rate (orange line) on this plot. Delay time distributions with even steeper power law slopes  $\alpha < -2$  would be even more similar to the LGRB rate, and become essentially indistinguishable from one another.

We compare these predicted merger rates to the measured BBH merger rate as a function of redshift, as inferred by Bavera et al. (2022a) from GWTC-3 observations. Bavera et al. (2022a) perform a hierarchical Bayesian fit to the BBH mass, spin and redshift distributions, fitting a Madau & Dickinson (2014)-like model to the BBH rate as a function of redshift while also allowing the BBH spin distribution to evolve with redshift. This measured BBH merger rate is shown in Fig. 1 with the purple line denoting the median and shaded bands denoting 68% credible intervals (right axis). Note that the right axis (BBH merger rate) is scaled by some constant factor with respect to the left axis (corresponding to all other curves) for ease of comparison. We define the constant scaling factor  $f$  between the BBH progenitor formation rate and the LGRB rate:

$$f \equiv \mathcal{R}_f / \mathcal{R}_{\text{LGRB}}. \quad (3)$$

This scaling factor accounts for the possibility that not all LGRBs evolve into merging BBH. Additionally, there may be BBH mergers that did not evolve from LGRBs (so that  $f$  may be larger than 1). Eq. 3 simply assumes that the ratio between the BBH progenitor formation rate and the LGRB rate is constant across redshift.

Looking at Fig. 1, we can see that the LGRB rate with a power-law delay time distribution given by  $\alpha = -0.96$  and  $\tau_{\min} = 10$  Myr (red curve), scaled by a factor  $f \approx 0.05$ , matches the BBH merger rate well. In the following, we make this comparison statistically rigorous.

## 2.2. Inferring the delay time distribution parameters

Our goal is to infer the delay time distribution parameters  $\alpha$ ,  $\tau_{\min}$  and the scaling factor  $f$ . For each combination of  $\alpha$ ,  $\tau_{\min}$ ,  $f$ , and LGRB rate parameters  $\theta_{\text{LGRB}}$ , we calculate  $\mathcal{R}_m(t_L | \alpha, \tau_{\min}, f, \theta_{\text{LGRB}})$  by numerically integrating Eq. 1 on a grid with step size  $d\tau = 1$  Myr. The  $\theta_{\text{LGRB}}$  parameters, which define  $\mathcal{R}_{\text{LGRB}}$ , are measured by Ghirlanda & Salvaterra (2022) and marginalized over in our analysis.

We then quantify the similarity between any given  $\mathcal{R}_m(t_L | \alpha, \tau_{\min}, f, \theta_{\text{LGRB}})$  curve and the measured BBH merger rate  $\mathcal{R}_{\text{BBH}}(t_L)$  following the method in Fishbach & Kalogera (2021). We first take the BBH merger rate at  $z = 0$  and  $z = 1$  (the highest merger redshift probed by GWTC-3) from the population fit of Bavera et al. (2022a) and apply a 2-dimensional Kernel Density Esti-

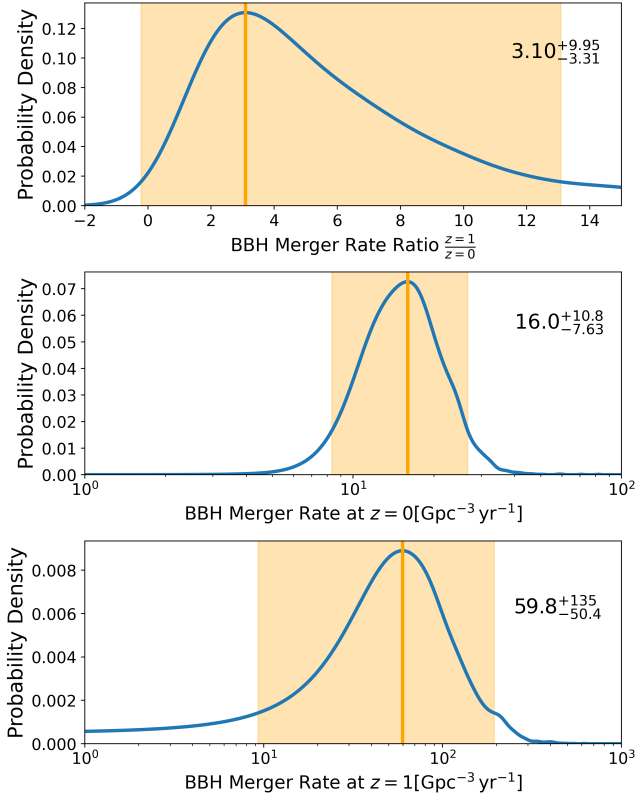


**Figure 2.** BBH merger rate at  $z = 0$  (middle panel),  $z = 1$  (lower panel) and the ratio between the merger rate at  $z = 1$  and  $z = 0$  (top panel) as inferred by [Bavera et al. \(2022a\)](#) using GWTC-3 observations. We apply a KDE to their population posterior samples. We report the maximum posterior value and the 90% highest density posterior intervals (HDPI), shown in orange.

mation (KDE). The posterior probability density functions of the BBH merger rate at  $z = 0$ ,  $z = 1$ , and the ratio  $\mathcal{R}_{\text{BBH}}(z = 1)/\mathcal{R}_{\text{BBH}}(z = 0)$  are shown in Fig. 2. The shape of the BBH merger rate is captured by the ratio  $\mathcal{R}_{\text{BBH}}(z = 1)/\mathcal{R}_{\text{BBH}}(z = 0)$ , and this carries information about the shape of the delay time distribution (i.e.  $\alpha$  and  $\tau_{\text{min}}$ ). Meanwhile, the amplitude of the BBH merger rate carries information about the amplitude of the progenitor formation rate (i.e.  $f$ ). This is illustrated in Fig. 3, which shows the 2-dimensional KDE of the BBH merger rate at  $z = 0$  and  $z = 1$ , overlaid with example  $\mathcal{R}_m$  values for various  $\alpha$  and  $f$  (fixing  $\tau_{\text{min}} = 10$  Myr and  $\theta_{\text{LGRB}}$  to the maximum likelihood value from [Ghirlanda & Salvaterra 2022](#)). Steeper delay time distributions (more negative  $\alpha$ ) correspond to a merger rate that increases faster with increasing redshift, i.e. larger ratios  $\mathcal{R}_{\text{BBH}}(z = 1)/\mathcal{R}_{\text{BBH}}(z = 0)$ . Curves of constant  $\alpha$  correspond to constant  $\mathcal{R}_{\text{BBH}}(z = 1)/\mathcal{R}_{\text{BBH}}(z = 0)$  and appear as lines in Fig. 3. Without making any prior assumptions on  $f$ , we can estimate  $\alpha$  based on the slope

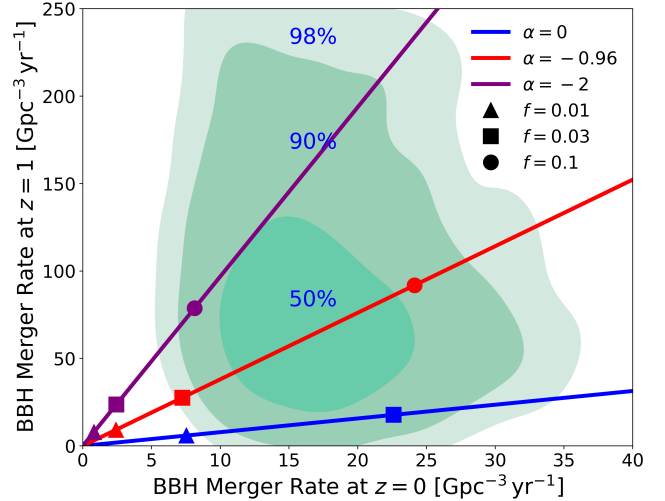


**Figure 3.** The BBH merger rate at redshift  $z = 0$  and  $z = 1$ , as inferred by [Bavera et al. \(2022a\)](#) and estimated here with a 2D KDE (green). Contours enclose regions of 50%, 90% and 98% probability. Blue, red and purple lines show power-law predictions for the BBH merger rate under different power-law delay time distributions with slope  $\alpha$  and  $\tau_{\text{min}} = 10$  Myr, assuming that the progenitor formation rate traces the best-fit LGRB rate from [Ghirlanda & Salvaterra \(2022\)](#). A delay time distribution with  $\alpha = -0.96$  (red) crosses the highest probability region. The circles, squares and triangles represents  $f$  values (the ratio between the BBH formation rate and the LGRB rate) of 0.1, 0.03 and 0.01.

of the inferred BBH merger rate function from  $z = 0$  to  $z = 1$ . From Fig. 3, we see that  $\alpha = -0.96$  is favored by the GW data because it passes through the highest probability region of the KDE. Meanwhile, increasing  $f$  increases the merger rate at all redshifts, corresponding to points further away from the origin in Fig. 3.

Following [Fishbach & Kalogera \(2021\)](#), we calculate a likelihood for any combination of delay time distribution and progenitor formation rate parameters by evaluating the 2-dimensional BBH merger rate KDE of Fig. 3 at the corresponding  $\mathcal{R}_m(z = 0|\alpha, \tau_{\text{min}}, f, \theta_{\text{LGRB}})$  and  $\mathcal{R}_m(z = 1|\alpha, \tau_{\text{min}}, f, \theta_{\text{LGRB}})$  values. We evaluate this likelihood on a grid of  $\alpha$  and  $f$  values. By default, we fix  $\tau_{\text{min}} = 10$  Myr (the typical minimum delay time predicted from population synthesis because it roughly corresponds to the lifetime of massive stars<sup>1</sup>). We marginalize over the uncertainty in the LGRB rate

<sup>1</sup> The delay time distributions predicted by population synthesis usually refer to the time between the birth of the progenitor star and the merger of the BBH. Here, we consider delay times between the birth of a BH (produced by the LGRB) and its merger in a BBH. This is shorter by  $\sim 10$  Myr (the typical massive star lifetime) than the traditional delay time distribution, which is too short a timescale to noticeably affect our results.



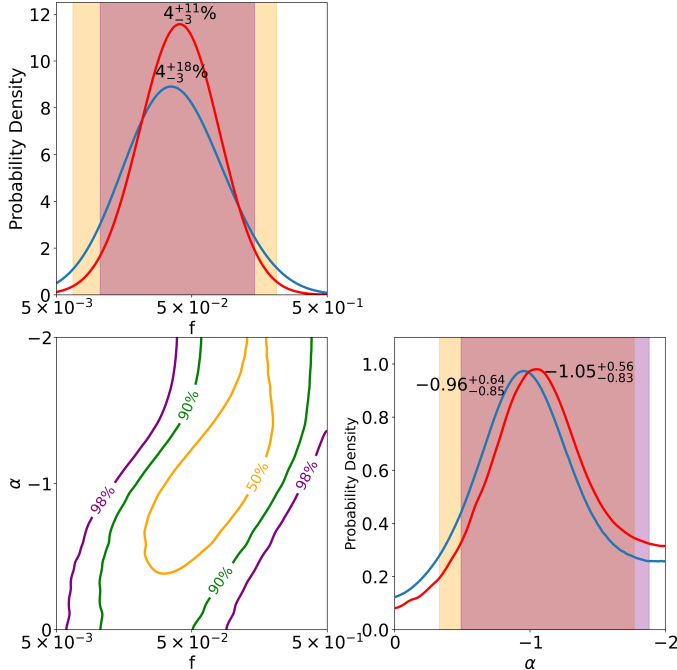


**Figure 4.** Bottom left: joint posterior on BBH delay time and formation rate parameters  $\alpha$  and  $f$ , fixing  $\tau_{\min} = 10$  Myr. Contours enclose 50%, 90%, and 98% posterior probability. Upper left: Posterior probability density for  $f$ , marginalizing over  $\alpha$  with a flat prior (blue curve, with orange band denoting 90% HPDI) or fixing to the maximum likelihood value of  $\alpha$  (red curve, with purple band denoting 90% HDPI). Bottom Right: Posterior probability density for  $\alpha$ , marginalizing over  $f$  with a flat-in-log prior (blue curve, with orange band denoting 90% HPDI) or fixing  $f$  to its maximum likelihood value (red curve, with purple band denoting 90% HPDI).

inferred by Ghirlanda & Salvaterra (2022) with a Monte Carlo average over 100  $\theta_{\text{LGRB}}$  samples. Because we do not have access to the full posterior distributions, we draw  $\theta_{\text{LGRB}}$  from the 1-dimensional credible regions reported by Ghirlanda & Salvaterra (2022), neglecting multi-dimensional correlations. This is a conservative estimate of the uncertainty in  $\mathcal{R}_{\text{LGRB}}$ .

From the likelihood over  $\alpha$  and  $f$ , we calculate the posterior according to Bayes’ theorem, choosing a flat prior on  $\alpha$  and a flat-in-log prior on  $f$ . (Power-law slopes steeper than -2 produce merger rates that are virtually indistinguishable; see Fig. 1.) We present the resulting posterior on  $\alpha$  and  $f$  in the following section. We also discuss the joint posterior between  $\tau_{\min}$  and  $\alpha$ , assuming flat priors on both parameters.

### 3. RESULTS

Figure 4 shows the joint posterior over the delay time distribution power-law slope  $\alpha$  and the relative amplitude of the progenitor formation rate  $f$ . We also show

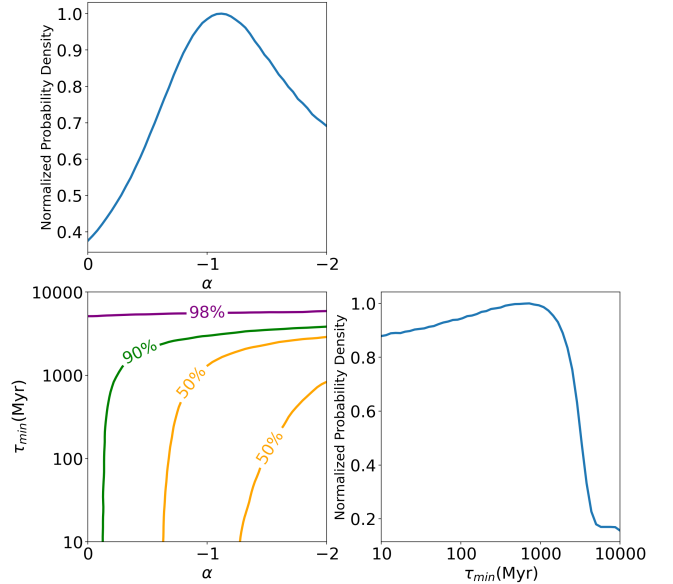


**Figure 5.** Joint posterior on delay time distribution parameters  $\alpha$  and  $\tau_{\min}$  (bottom left), with marginalized posteriors on each parameter in the top left and bottom right. Longer minimum delay times  $\tau_{\min}$  favors steeper (more negative) power law slopes  $\alpha$ , while very long  $\tau_{\min} \gtrsim 4$  Gyr is not favored by any value of  $\alpha$ . The inferred value of  $f$  corresponding to each delay time distribution is roughly constant along the highest posterior probability ( $\alpha, \tau_{\min}$ ) contour.

the one-dimensional posteriors on  $\alpha$  and  $f$ , marginalizing over the other variable (red curves) or fixing the other variable to its maximum likelihood value (blue curve). We summarize our measurements with 90% highest density posterior intervals (HDPI).

Consistent with the results suggested by Fig. 1 and Fig. 3, we find  $\alpha = -0.96^{+0.64}_{-0.85}$  (marginalizing over  $f$ ) and  $f = 0.04^{+0.18}_{-0.03}$  (marginalizing over  $\alpha$ ). In other words, assuming a progenitor formation rate proportional to the LGRB rate, the GWTC-3 data prefer a nearly flat-in-log delay time distribution ( $\alpha \approx -1$ ). The BBH progenitor formation rate is likely  $\approx 4\%$  of the LGRB rate.

These results correspond to a fixed minimum delay time of  $\tau_{\min} = 10$  Myr. In Fig. 5, we show the joint posterior between  $\tau_{\min}$  and  $\alpha$ , assuming a flat prior on  $\tau_{\min}$  between 10 Myr–10 Gyr. For this result, we consider only the shape of the merger rate captured by the ratio  $\mathcal{R}_m(z=1)/\mathcal{R}_m(z=0)$  and ignore the amplitude, thereby factoring out any dependence on  $f$ . We see that even when marginalizing over the minimum delay time, the posterior for  $\alpha$  peaks around  $\alpha \approx -1$ . Nevertheless, as seen by the joint posterior, larger  $\tau_{\min}$  imply steeper power-law slopes, because the delay time distribution compensates to keep the same average delay time. Marginalizing over  $\alpha$ , it is hard to distinguish be-

tween values of  $\tau_{\min}$  as long as  $\tau_{\min} \lesssim 1$  Gyr. Minimum delay times larger than 4 Gyr are ruled out, because they would imply a BBH merger rate that peaks at  $z < 1$ , which is not consistent with the GW data. Although we do not simultaneously fit for  $f$ ,  $\alpha$  and  $\tau_{\min}$ , we check that the maximum likelihood value of  $f$  is constant along the high-probability region in the joint  $\alpha$  and  $\tau_{\min}$  posterior, and therefore our conclusions about  $f$  are unaffected by varying  $\tau_{\min}$  alongside  $\alpha$ .

We also consider the scenario proposed by [Bavera et al. \(2022b\)](#) in which LGRBs only give rise to the subset of BBH mergers with moderately large spins that are aligned with the orbital angular momentum. Specifically, [Bavera et al. \(2022b\)](#) consider BBH mergers with effective inspiral spin  $\chi_{\text{eff}} > 0.2$ . The fraction of BBH mergers with  $\chi_{\text{eff}} > 0.2$  is small, but may increase with increasing redshift ([Biscoveanu et al. 2022](#); [Bavera et al. 2022a](#)). By modeling a redshift-dependent  $\chi_{\text{eff}}$  distribution, the population inference of [Bavera et al. \(2022a\)](#) provides a measurement of the rate of BBH mergers with  $\chi_{\text{eff}} > 0.2$  as a function of redshift. We repeat our analysis using this “ $\chi_{\text{eff}} > 0.2$ ” BBH merger rate instead of the total BBH merger rate. The resulting inference on  $\alpha$  and  $f$  is shown in Fig. 6. Under the assumption that only these high-spinning BBH mergers come from LGRBs, we estimate that their progenitor formation rate is most likely  $< 1\%$  of the LGRB rate. Meanwhile, the delay time distribution remains consistent with a flat-in-log distribution, but favors steeper power-law slopes, railing against the prior boundary at  $\alpha = -2$ . This is because the slope of the high-spin BBH merger rate agrees with the slope of the LGRB rate from redshift 0 to 1, requiring essentially no delay times. Within our prior boundaries, we constrain  $\alpha < -0.64$  at 90% credibility. This may imply that BBH mergers with high aligned spins experience shorter delay times than slowly-spinning BBH systems, which is consistent with predictions that spinning BBHs originate in tighter binary orbits that merge faster (e.g. [Bavera et al. 2022a](#)).

#### 4. DISCUSSION AND CONCLUSIONS

By comparing the redshift evolution of LGRBs and BBH mergers, we find that the BBH merger rate is consistent with tracing a scaled LGRB rate with a flat-in-log delay time distribution (with a best fit power-law slope of  $\alpha = -0.96$ , under which 60% of BBH mergers occur within 1 Gyr of formation). This delay time distribution is consistent with theoretical predictions for the formation of BBH mergers from several channels, including isolated binary evolution and dynamical assem-

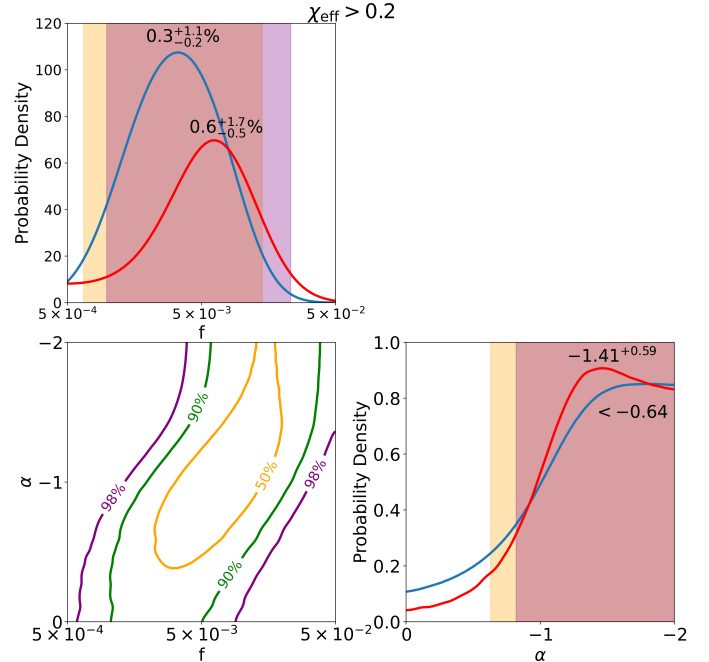


**Figure 6.** Same as Fig. 4, but using the subpopulation of BBH mergers with  $\chi_{\text{eff}} > 0.2$  rather than the full BBH population, assuming that LGRBs produce spinning BHs. Compared to Fig. 4, smaller values of  $f$  and more negative values of  $\alpha$  are preferred in this case. The rate of BBH mergers with  $\chi_{\text{eff}} > 0.2$  over the measured range  $0 < z < 1$  is consistent with tracing the best-fit LGRB rate, so we infer steep delay time distributions peaking at our prior boundary  $\alpha = -2$ .

bly in dense star clusters<sup>2</sup> ([O’Shaughnessy et al. 2010](#); [Dominik et al. 2012](#); [Mapelli et al. 2017](#); [Di Carlo et al. 2020](#); [Fishbach & van Son 2023](#); [Ye & Fishbach 2024](#)). Previous work has assumed that the BBH progenitor formation rate traces the SFR (often with some metallicity dependence), in which case significantly steeper power-law slopes are preferred. The consistency between our recovered delay time distribution and theoretical predictions suggests that the LGRB rate is a better tracer of the BBH progenitor formation rate than the SFR, at least under the previously used assumptions for the metallicity-specific SFR and the metallicity dependence of BBH progenitors.

Nevertheless, our results do not definitively prove that LGRBs are progenitors to BBH mergers. We find that BBH progenitors are much rarer than LGRBs, accounting for only  $4^{+18}_{-3}\%$  of the LGRB rate. This is smaller although not entirely inconsistent with [Bavera et al. \(2022b\)](#), who report that 20–85% of LGRBs may be pro-

<sup>2</sup> For BBH assembly in star clusters, the delay time is defined as the time between cluster formation and BBH merger.

duced by the progenitors of BBH systems. However, if LGRBs produce spinning BHs, we find that this fraction is much smaller:  $0.3_{-0.2}^{+1.1}\%$ . Nevertheless, [Gottlieb et al. \(2023\)](#) and [Jacquemin-Ide et al. \(2024\)](#) have recently argued that only moderate rotation of the stellar core is necessary to power an LGRB, and that the LGRB itself may spin down the resulting BH. The fact that so few BBH mergers have large aligned spins may lend support to this argument.

Rather than a direct relationship between LGRBs and BBH progenitors, it may instead be that both populations trace the low-metallicity SFR with similar metallicity thresholds. In this case, it is still convenient to use LGRBs as probes of the low-metallicity SFR, because they are detected out to high redshifts, whereas low-metallicity SFR occurs mainly in small, faint galaxies that are hard to directly observe. Rather than direct measurements of the SFR in these galaxies, [Mukherjee & Dizgah \(2022\)](#) proposed cross-correlating line intensity maps with BBH mergers in order to constrain the BBH delay time distribution, a promising technique once line-intensity mapping surveys reach completion. Future GRB, GW and galaxy data would enable us to better un-

derstand the metallicity-dependence of the LGRB and BBH populations and the reasons behind their similarities or differences, with implications for stellar collapse, supernova explosions and binary evolution. Combining asynchronous observations of gamma rays and gravitational waves provides a multi-messenger view of black hole lifecycles across cosmic history.

- 1 We thank Michael Zevin for helpful comments on the  
 2 manuscript. MF is supported by the Natural Sci-  
 3 ences and Engineering Research Council of Canada  
 4 (NSERC) under grant RGPIN-2023-05511. MF is  
 5 grateful to the Lorentz Center, the scientific organiz-  
 6 ers and the participants of the workshop “Gravita-  
 7 tional waves: a new ear on the chemistry of galaxies”  
 8 (29 April - 3 May 2024, [https://www.lorentzcenter.nl/  
 9 gravitational-waves-a-new-ear-on-the-chemistry-of-galaxies.  
 10 html](https://www.lorentzcenter.nl/gravitational-waves-a-new-ear-on-the-chemistry-of-galaxies.html)) for helpful discussions. This material is based  
 11 upon work supported by NSF’s LIGO Laboratory which  
 12 is a major facility fully funded by the National Science  
 13 Foundation.

## REFERENCES

- Abbott, R., Abbott, T. D., Acernese, F., et al. 2023, *Physical Review X*, 13, 041039, doi: [10.1103/PhysRevX.13.041039](https://doi.org/10.1103/PhysRevX.13.041039)
- Acernese, F., Agathos, M., Agatsuma, K., et al. 2015, *Classical and Quantum Gravity*, 32, 024001, doi: [10.1088/0264-9381/32/2/024001](https://doi.org/10.1088/0264-9381/32/2/024001)
- Akutsu, T., Ando, M., Arai, K., et al. 2021, *Progress of Theoretical and Experimental Physics*, 2021, 05A101, doi: [10.1093/ptep/ptaa125](https://doi.org/10.1093/ptep/ptaa125)
- Arcier, B., & Atteia, J.-L. 2022, *ApJ*, 933, 17, doi: [10.3847/1538-4357/ac6604](https://doi.org/10.3847/1538-4357/ac6604)
- Astropy Collaboration, Robitaille, T. P., Tollerud, E. J., et al. 2013, *A&A*, 558, A33, doi: [10.1051/0004-6361/201322068](https://doi.org/10.1051/0004-6361/201322068)
- Astropy Collaboration, Price-Whelan, A. M., Lim, P. L., et al. 2022, *ApJ*, 935, 167, doi: [10.3847/1538-4357/ac7c74](https://doi.org/10.3847/1538-4357/ac7c74)
- Bavera, S. S., Fishbach, M., Zevin, M., Zapartas, E., & Fragos, T. 2022a, *A&A*, 665, A59, doi: [10.1051/0004-6361/202243724](https://doi.org/10.1051/0004-6361/202243724)
- Bavera, S. S., Fragos, T., Zapartas, E., et al. 2022b, *A&A*, 657, L8, doi: [10.1051/0004-6361/202141979](https://doi.org/10.1051/0004-6361/202141979)
- Belczynski, K., Dominik, M., Bulik, T., et al. 2010, *ApJL*, 715, L138, doi: [10.1088/2041-8205/715/2/L138](https://doi.org/10.1088/2041-8205/715/2/L138)
- Biscoveanu, S., Callister, T. A., Haster, C.-J., et al. 2022, *ApJL*, 932, L19, doi: [10.3847/2041-8213/ac71a8](https://doi.org/10.3847/2041-8213/ac71a8)
- Boesky, A., Broekgaarden, F. S., & Berger, E. 2024, arXiv e-prints, arXiv:2405.01623, doi: [10.48550/arXiv.2405.01623](https://doi.org/10.48550/arXiv.2405.01623)
- Chruślińska, M. 2024, *Annalen der Physik*, 536, 2200170, doi: [10.1002/andp.202200170](https://doi.org/10.1002/andp.202200170)
- Di Carlo, U. N., Mapelli, M., Giacobbo, N., et al. 2020, *MNRAS*, 498, 495, doi: [10.1093/mnras/staa2286](https://doi.org/10.1093/mnras/staa2286)
- Dominik, M., Belczynski, K., Fryer, C., et al. 2012, *ApJ*, 759, 52, doi: [10.1088/0004-637X/759/1/52](https://doi.org/10.1088/0004-637X/759/1/52)
- . 2013, *ApJ*, 779, 72, doi: [10.1088/0004-637X/779/1/72](https://doi.org/10.1088/0004-637X/779/1/72)
- Fishbach, M., & Kalogera, V. 2021, *ApJL*, 914, L30, doi: [10.3847/2041-8213/ac05c4](https://doi.org/10.3847/2041-8213/ac05c4)
- Fishbach, M., & van Son, L. 2023, *ApJL*, 957, L31, doi: [10.3847/2041-8213/ad0560](https://doi.org/10.3847/2041-8213/ad0560)
- Ghirlanda, G., & Salvaterra, R. 2022, *ApJ*, 932, 10, doi: [10.3847/1538-4357/ac6e43](https://doi.org/10.3847/1538-4357/ac6e43)
- Gottlieb, O., Jacquemin-Ide, J., Lowell, B., Tchekhovskoy, A., & Ramirez-Ruiz, E. 2023, *ApJL*, 952, L32, doi: [10.3847/2041-8213/ace779](https://doi.org/10.3847/2041-8213/ace779)
- Jacquemin-Ide, J., Gottlieb, O., Lowell, B., & Tchekhovskoy, A. 2024, *ApJ*, 961, 212, doi: [10.3847/1538-4357/ad02f0](https://doi.org/10.3847/1538-4357/ad02f0)
- Klencki, J., Moe, M., Gladysz, W., et al. 2018, *A&A*, 619, A77, doi: [10.1051/0004-6361/201833025](https://doi.org/10.1051/0004-6361/201833025)

- LIGO Scientific Collaboration, Aasi, J., Abbott, B. P., et al. 2015, *Classical and Quantum Gravity*, 32, 074001, doi: [10.1088/0264-9381/32/7/074001](https://doi.org/10.1088/0264-9381/32/7/074001)
- MacFadyen, A. I., & Woosley, S. E. 1999, *ApJ*, 524, 262, doi: [10.1086/307790](https://doi.org/10.1086/307790)
- Madau, P., & Dickinson, M. 2014, *ARA&A*, 52, 415, doi: [10.1146/annurev-astro-081811-125615](https://doi.org/10.1146/annurev-astro-081811-125615)
- Madau, P., & Fragos, T. 2017, *ApJ*, 840, 39, doi: [10.3847/1538-4357/aa6af9](https://doi.org/10.3847/1538-4357/aa6af9)
- Mandel, I., & Farmer, A. 2022, *PhR*, 955, 1, doi: [10.1016/j.physrep.2022.01.003](https://doi.org/10.1016/j.physrep.2022.01.003)
- Mapelli, M. 2020, *Frontiers in Astronomy and Space Sciences*, 7, 38, doi: [10.3389/fspas.2020.00038](https://doi.org/10.3389/fspas.2020.00038)
- Mapelli, M., Giacobbo, N., Ripamonti, E., & Spera, M. 2017, *MNRAS*, 472, 2422, doi: [10.1093/mnras/stx2123](https://doi.org/10.1093/mnras/stx2123)
- Mapelli, M., Giacobbo, N., Santoliquido, F., & Artale, M. C. 2019, *MNRAS*, 487, 2, doi: [10.1093/mnras/stz1150](https://doi.org/10.1093/mnras/stz1150)
- Mukherjee, S., & Dizgah, A. M. 2022, *ApJL*, 937, L27, doi: [10.3847/2041-8213/ac903b](https://doi.org/10.3847/2041-8213/ac903b)
- O'Shaughnessy, R., Kalogera, V., & Belczynski, K. 2010, *ApJ*, 716, 615, doi: [10.1088/0004-637X/716/1/615](https://doi.org/10.1088/0004-637X/716/1/615)
- Palmerio, J. T., Vergani, S. D., Salvaterra, R., et al. 2019, *A&A*, 623, A26, doi: [10.1051/0004-6361/201834179](https://doi.org/10.1051/0004-6361/201834179)
- Perley, D. A., Tanvir, N. R., Hjorth, J., et al. 2016a, *ApJ*, 817, 8, doi: [10.3847/0004-637X/817/1/8](https://doi.org/10.3847/0004-637X/817/1/8)
- Perley, D. A., Krühler, T., Schulze, S., et al. 2016b, *ApJ*, 817, 7, doi: [10.3847/0004-637X/817/1/7](https://doi.org/10.3847/0004-637X/817/1/7)
- Peters, P. C. 1964, *Physical Review*, 136, 1224, doi: [10.1103/PhysRev.136.B1224](https://doi.org/10.1103/PhysRev.136.B1224)
- Planck Collaboration, Aghanim, N., Akrami, Y., et al. 2020, *A&A*, 641, A6, doi: [10.1051/0004-6361/201833910](https://doi.org/10.1051/0004-6361/201833910)
- Rodriguez, C. L., & Loeb, A. 2018, *ApJL*, 866, L5, doi: [10.3847/2041-8213/aae377](https://doi.org/10.3847/2041-8213/aae377)
- Santoliquido, F., Mapelli, M., Giacobbo, N., Bouffanais, Y., & Artale, M. C. 2021, *MNRAS*, 502, 4877, doi: [10.1093/mnras/stab280](https://doi.org/10.1093/mnras/stab280)
- Schiebelbein-Zwack, A., & Fishbach, M. 2024, *ApJ*, 970, 128, doi: [10.3847/1538-4357/ad5353](https://doi.org/10.3847/1538-4357/ad5353)
- Turbang, K., Lalleman, M., Callister, T. A., & van Remortel, N. 2024, *ApJ*, 967, 142, doi: [10.3847/1538-4357/ad3d5c](https://doi.org/10.3847/1538-4357/ad3d5c)
- Vergani, S. D., Salvaterra, R., Japelj, J., et al. 2015, *A&A*, 581, A102, doi: [10.1051/0004-6361/201425013](https://doi.org/10.1051/0004-6361/201425013)
- Vijaykumar, A., Fishbach, M., Adhikari, S., & Holz, D. E. 2023, arXiv e-prints, arXiv:2312.03316, doi: [10.48550/arXiv.2312.03316](https://doi.org/10.48550/arXiv.2312.03316)
- Woosley, S. E. 1993, *ApJ*, 405, 273, doi: [10.1086/172359](https://doi.org/10.1086/172359)
- Ye, C. S., & Fishbach, M. 2024, *ApJ*, 967, 62, doi: [10.3847/1538-4357/ad3ba8](https://doi.org/10.3847/1538-4357/ad3ba8)